Memoirs of the School of Engineering Okayama University Vol. 11, No. 1, July 1976

Anomalous Electric Fields in n-InSb under High Magnetic Fields. I-Experiment

Tadao ISHII and Mitsuharu DOI *

Synopsis

An investigation was made of the anomalous electric field in its various aspects in n-type InSb subjected to strong magnetic field at 77K and 273K, which lead to the conclusion that no open contradiction arose between a part of the present observations and the predictions attainable from Yoshida's model of semimetals. There remained, however, the other part of the experimental results unexplained, being rather natural since an inner property of indium antimonide does not seem so simple comparing with the compensated metals, bismuth and antimony. Especially as for the mechanism of an inversion phenomenon of the polarity of a negative anomalous field at a critical pulse current, we have no available theory to explain at present stage.

1. Introduction

Anomalous electric fields have been reported by Morimoto and Yoshida in bismuth and antimony in high magnetic fields at low temperature, which are characterized by the form of negative dip and positive hump in the angular dependence diagram of the potential difference.[1-3] Subsequently the analogous effects have been observed also in n-InSb by Morimoto and his co-workers, confirming that role of holes is essentially important.[4,5] Recently Yoshida illustrated the matters in the semimetals by the current trajectory and the equipotential line under the influence of magnetic field.[6] Both phenomena in the semimetals and the narrow-gap semiconductor seem to originate from the same mechanism. The phenomena, however, seemed not satisfactorily explained, mainly because of smallness of the amount of available data.

* Department of Electronics

Experimental studies of the anomalous electric fields in n-InSb will be made, in the present paper, whose results are tried to interpret by use of Yoshida's model as possible. It is shown, however, that there remain unexplained observations within the model. It may be attributable to the difference of the degree of compensation, conditions of the surfaces and so on, being not always covered with the scope of Yoshida's calculation.

2. Experimental Procedures

Specimens of rectangular parallelpiped with various sizes were prepared by cutting out single-crystal blocks and a wafer produced by Sumitomo Electric Industries with a wire-slicing machine. The subsequent lapping were made by use of 3 and 8 micron abrasive, but we never take care of degrees of the finished surfaces since the surfaces finished with each of powders give no discriptive differences on the effects concerned.

Two kinds of potential probes were attempted; one is symbolized and called as Au-probe, where gold leads of 0.1 mm diameter were welded in a dotted way to a side surface by a discharge method in the contact diameter about 0.4 mm, while the other is W-probe where a pair of tungsten leads of point diameters about 0.1 mm with their spacing about 1 mm were pushed against a side surface. As the current electrodes, we tried two ways; one of them is the same as in Au-probe of the gold leads described above, welded to each center of the end surfaces, while the other is the method that the gold wires are soldered to the electrodes where indium were electroplated on all the end surfaces. The former will be called as Au-electrode and the latter as In-electrode.

Table I. Geometrical and physical parameters of specimens in unit of mm (dimension), $cm^2/V\cdot sec$ (mobility) and cm^{-3} (density).

specimen(*T)	x	y	z	mobility**	density**	probe/electrode
#1 (273)	1.61 [211]or[110]	1.57 [110]or[211]	8.67 [111]	6.8×10^4 / 3.8×10^5	2.2×10^{16} / 2.2×10^{14}	Au- /Au-
#2 (273, 77)	1.88 [211]or[111]	1.85 [111]or[211]	9.62 [110]	6.9×10^4 / 2.5×10^5	2.2×10^{16} / 2.3×10^{15}	Au- /Au-
#3 (273)	2.07 [110]	1.46 [111]	19.74 [211]	/ 3.0×10^5	/ 1.6×10^{14}	W - /In-
#4 (273)	2.01(2.01)	1.50(1.49)	15.23			W(Au)-/Au-
#5 (273)	2.00(1.99)***	1.47(1.46)	14.91			W(Au)-/In-
#6 (273)	2.14	1.48	15.71			W(Au)-/In-

* The physical constants and crystallographic directions are same through

#3-#6, and (T) means the temperature in measurement.

** The upper values are at 300K and the lower values at 77K.

*** The Au-probe is used only for a specimen of the size within the parenthesis while the W-probe is used for both.

Specimen dimensions, axes, physical constants and methods of probe and current electrode are listed in Table I, where the current flow is taken parallel to the z-axis and the magnetic field (0-12.5KG) placed in the y-z plane makes an angle θ with the z-axis. Particularly for the specimen #1 and #2, ten Au-probes were attached on a side surface (x-z plane) along its median line in order to survay the potential distribution, and seven Au-probes on each side surface (x-z and y-z plane), respectively.

The potential difference between the terminals i and j, $V_{zz}^{\alpha}(ij)$ specified in Fig.1, is examined at the two side surfaces perpendicular to each other; α=x or y indicates the direction normal to the relevant surface, z the direction of the current flow. In the present experiment, the angular dependence of V_{zz}^{x} or V_{zz}^{y} is studied by rotating z-direction of specimen around the magnetic field direction as in Fig.1, under various conditions: Constant currents of some mA at 273K or 77K are supplied to the specimens, pulse currents, on the other hand, of about 0.5-6 A with about 40 μsec width and repetition rate of 1 Hz are also supplied to see the behavior of anomalous electric field.

3. Experimental Results

3.1 Angular dependence of the anomalous potential difference

The main diagram of Fig.1 shows the typical angular dependence of the potential difference, where in the solid curve clear spike-shaped dips marked with letters d+ and d- are observed at angles θ_{d+}=27° and θ_{d-}=-153°. In the range of angles where negative dips are observed, the direction of electric field is opposite to that of total current flow. It is also seen that humps denoted by letters h+ and h- appear at angles θ_{h+}=48° and θ_{h-}=-128°. Such a dip and a hump usually appear in a couple but these are not always pointed out. On the other hand, the dashed curve, the potential difference $V_{zz}^{x}(1'2')$ does also exhibit unclear hump and negative dip,as is the case of ref.7, at θ_{d+}=12° and θ_{h+}=40° respectively, which could not be observed in the semimetals.[2,3] The spacings from the anode to the terminal 1 and the terminal 2 are 1.09 mm and 2.28 mm respectively, and from the anode to the terminal 1' and the terminal 2' are 0.98 mm and 2.16 mm respectively.

The nature of such anomalous angular dependence curve having dips and humps is strongly affected by geometrical conditions such as specimen size, the location of potential probes and the state of potential probe and current electrode, as will be shown in the following subsections.

3.1.1 Patterns of angular dependence diagram

For the specimen #1 under the condition T=273K, H=12.5 KG and I=5 mA, the negative dip exists in $V^{y}_{zz}(i,i+1)$ at angle $\theta_d(i)$ for all i=1-9 (refer to the insert of Fig.1 for #2). Now let us pay attention to the terminal 9. The potential difference $V^{y}_{zz}(9,9\pm j)$ for j=1-4 have the negative dip but not for j≥5.

On the other hand, for #2 under the condition T=273K, H=12.5 KG and I=1 mA, $V^{y}_{zz}(i,i+1)$ at the middle points i=3 and 4 possess no negative dip while for $V^{x}_{zz}(i,i+1)$ only the terminals i=1' and 6' concern the negative dip. It should be noted, however, that both $V^{y}_{zz}(17)$ and $V^{x}_{zz}(1'7')$ have the negative dip although is the latter small when T=77K (see sec. 3.1.3): Even in this case we found no negative dip in $V^{x}_{zz}(2'6')$ at any angle θ. The above facts suggest that the negative dip occurs easier at 77K than at 273K, as having been ascertained by Morimoto in detail.[7] Here we illustrate Fig.2 as an example of the pattern deformation on temperature. The pattern itself makes small change. It can be also noticed that the pattern of angular dependence diagram does not change its shape so large with respect to magnetic field (Fig.3).

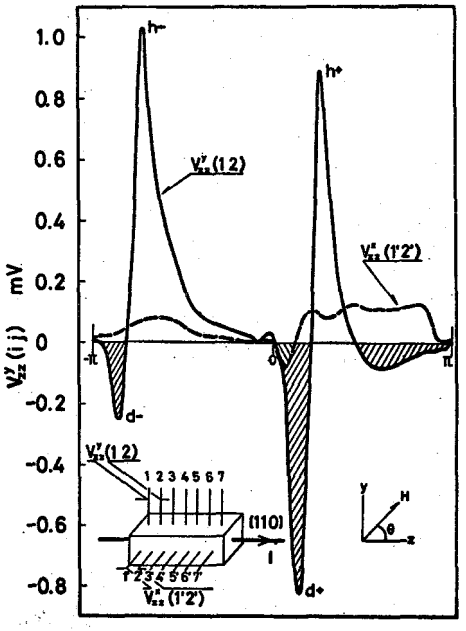

Fig.1 Angular dependence diagram of $V^{y}_{zz}(12)$ and $V^{x}_{zz}(1'2')$ for #2 at 77K with I=1 mA and H=12.5 KG.

On the contrary, position dependence of the pattern is quite characteristic.

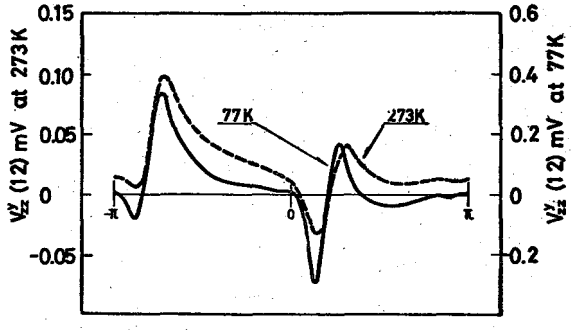

Fig.2 Angular dependence diagram of $V^{y}_{zz}(12)$ for #2 at 273K and 77K under I=1 mA and H=6000 G.

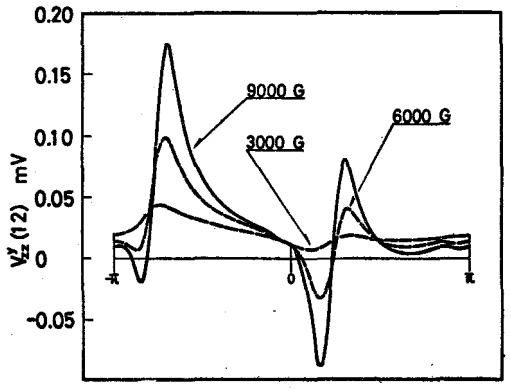

Fig.3 Angular dependence diagram of $V^y_{zz}(12)$ for #2 at 273K under I= 1 mA and H=3000, 6000 and 9000 G.

Fig.4 indicates rather symmetric patterns between solid and dashed curves with respect to θ=0°: The solid curve comes out from the potential difference $V^y_{zz}[1.54^-,0.90]$ and the dashed curve from $V^y_{zz}[1.41^+,0.91]$ for #4 under T=273K, H= 12.5 KG and I=3 mA. $\Delta\ell$ in $V^y_{zz}[\ell^+,\Delta\ell]$ is the spacing of a pair of tungsten probes used as the potential measurement at a position ℓ^+: ℓ^+ implies the distance between the anode and the nearer tungsten probe to it. The pattern measured at central position forms rather symmetric.

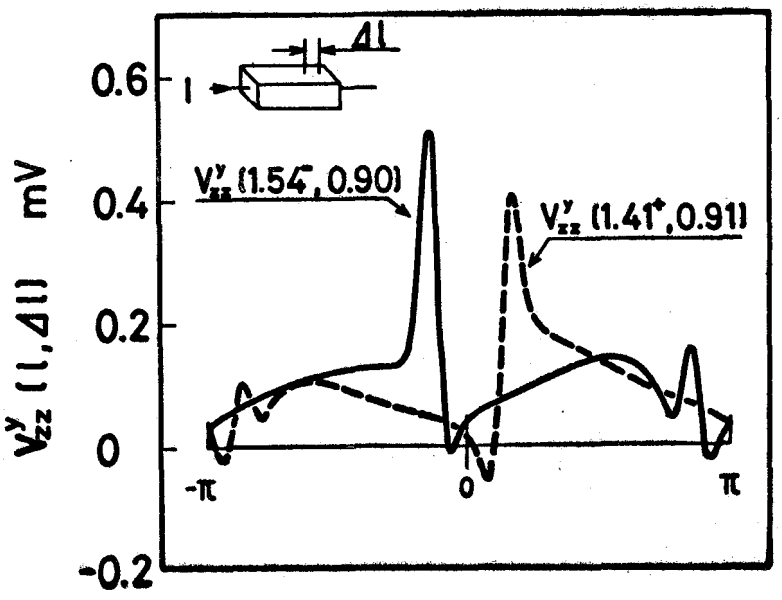

Fig.4 Angular dependence diagram of $V^y_{zz}[\ell,\Delta\ell]$ for #4 at 273K under I=3 mA and H=12.5 KG. A pair of tungsten probes with a spacing of $\Delta\ell$ are used as the potential measurement at a position ℓ; ℓ^+ means the distance between anode and nearer tungsten lead to it and ℓ^- the distance between cathode and nearer tungsten to it.

3.1.2 Magnetic field dependence of the voltage of dip and hump

We have checked up on the matter that the pattern of angular dependence diagram does not change its shape if the magnetic field varied in strength as shown in Fig.3. Let us take notice of the dip (d+) and hump (h-) in Fig.1 and measure the potential difference of $V^{y}_{zz}(12;d+)$ and $V^{y}_{zz}(12;h-)$ as a function of magnetic field. Fig.5 represents the magnetic field dependence of the potential difference for #2 under T=77K and I=1 mA. $V^{y}_{zz}(12;d+)=V^{y}_{zz}(12;h-)$ at zero magnetic field is 0.025 mV. At rather low magnetic field, $V^{y}_{zz}(12)$ is not correctly a function of H^2; $V^{y}_{zz}(12;d+)$ happens to depend on H^2 but $V^{y}_{zz}(12;h-)$ does not so. As for the above dip, we accumulate the eleven analogous data for I=1-100 mA and average over them to yield the field dependence H^2. At high field region, $V^{y}_{zz}(12)$ is linearly dependent on H. The value at which $V^{y}_{zz}(12;d+)$ intersects zero is H=1500 G (μH=3.7) which is common among the other ten data. Here it is pertinent to add that the current dependence of $V^{y}_{zz}(12;d+)$ with a parameter H presents the exact linearity to the current 100 mA.

3.1.3 Potential distribution

As we described in the beginning of sec. 3.1.1, the potential difference does not seem so simple. Fig.6 is an example of a family of potential distribution curves for #2 along the median line of the surface (V^{y}_{zz}), under T=77K, H=12.5 KG and I=1 mA. The potential level at the terminal 7 is taken zero except the dashed curve. $V^{y}_{zz}(17)$ at $\theta=-57°$ can be observed negative, and also $V^{y}_{zz}(26)$ at $\theta=-45°$. Furthermore it is figured out that the distinctive valleys positioned at the terminal 2 are shown in each solid curve with an only exception $\theta=-135°$, while for $\theta>0$ they turn a group of mountains as shown by the dashed line. On the other hand $V^{x}_{zz}(1'7')$ indicate negative but small as 0.01 mV.

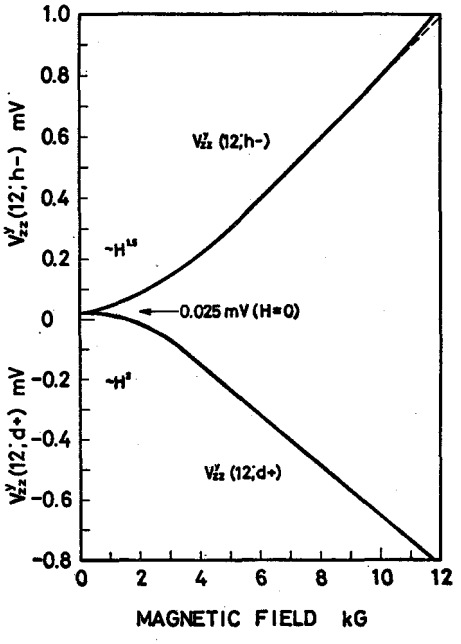

Fig.5 Magnetic field dependence of $V^{y}_{zz}(12;h-)$ and $V^{y}_{zz}(12;d+)$ for #2 at 77K under I=1 mA; the angles θ_{h-} and θ_{d+} shown in Fig.1 are selected.

3.2 Effects of size, probe and electrode

The studies have been done mainly with the samples #1 and #2, each of which has its length less than 10 mm. In these cases as we have seen, the negative dip has been detected between almost every two terminals. Here the

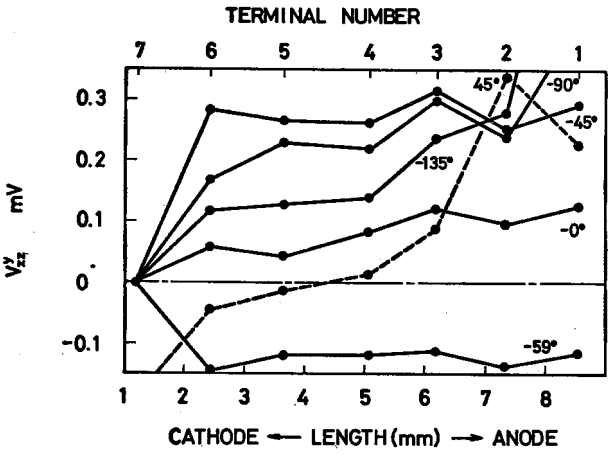

Fig.6 Potential variation along the median line of specimen surface.

specimens with sizes of 15-20 mm in length are investigated, where on the specimen #4 for instance the negative dip can not be detected at a position at least from 3.04 mm to 12.13 mm; both values are the distances from the cathode to the middle point of the potential probes. In adopting the symbol used in sec.3.1.1, 3.04 and 12.13 can be represented as $[2.59^{-},0.89]$ and $[11.63^{-},0.99]$, respectively.

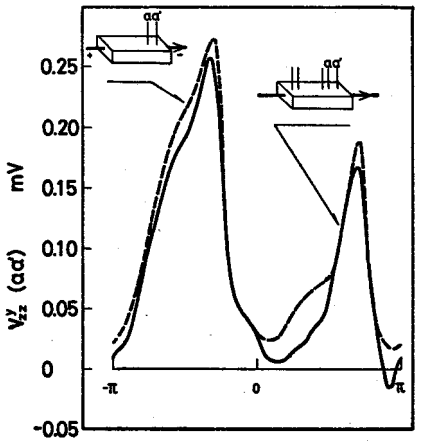

Fig.7 Probe effect of $V_{zz}^{y}(aa')$ for #5 at 273K under I=3 mA and H=12.5 KG. $V_{zz}^{y}(aa')$ with the other three probes other than the probes a and a' indicates the negative field but that without any probes does not.

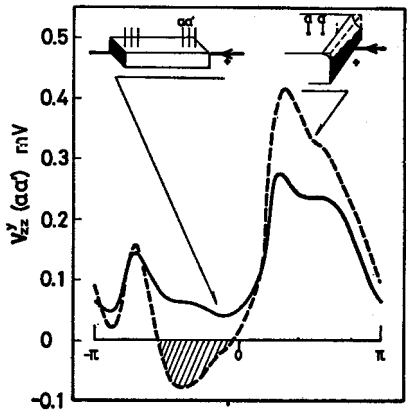

Fig.8 Angular dependence diagram of V(a a') for #6 at 273K under I=3 mA and H=12.5 KG. Potential probes and current electrodes are Au-probes and In-electrodes respectively.

If the end surfaces are all covered with indium contact, being the case of In-electrode, the negative dip does not appear at all over the side surfaces. This fact was well-ascertained in #3, #5 and #6, which may be equivalent to the case of semimetals that the anomalous electric fields become less conspicuous as the cross-section of a specimen is decreased.[3)]

It should be noted that the anomalous fields are not all intrinsic bulk effects because an interaction of the potential difference, say $V^{y}_{zz}(i,i+1)$, with the terminals $j\neq(i,i+1)$ happens to give the anomalous field. In Fig.7 is shown the above interaction. Only a pair of Au-probes [0.93^{-},0.61] at first are attached to measure V^{y}_{zz}[0.93^{-},0.61] and result in the dashed curve. At second step we add three terminals positioned at 2.16^{-}, 12.84^{-} and 13.58^{-} mm, then the negative dip comes out as in the solid curve. As for the specimen #6, six Au-probes are welded: Only the first pairs [14.54^{-}, 0.69] on the surface yields the positive field, and then after the second pairs [0.69^{-},0.79] are welded the measurement indicates also positive field. The fifth terminal attachment at 2.31^{-} mm and the two measurements of V^{y}_{zz}[0.69^{-},0.79] and V^{y}_{zz}[14.54^{-},0.69], and the sixth terminal attachment at 13.72^{-} mm and the three measurements V^{y}_{zz}[14.54^{-},0.69], V^{y}_{zz}[13.72^{-},0.82] and V^{y}_{zz}[1.48^{-},0.83] were subsequently made to result in the positive fields. Finally when we chipped a part of the anode edge, however, the large negative dip has appeared in V^{y}_{zz}[13.72^{-}, 0.82] but not at other positions (Fig.8).

3.3 Pulse mode operation

The absolute intensity of $V^{y}_{zz}(12)$ at angle θ_{d+} in Fig.1 has been linearly proportional to the current within 100 mA. This means that the current does not change a polarity of the potential difference far from the cases of magnetic field and temperature. What is the matter in the high electric field case? The pulse currents of 40 μsec-width and one Hz are supplied for #2 at 77K under H=12.5 KG and θ=-59°, where the voltage wave form begins to deform its shape at about 2A (Fig.9). At around 4.6 A the negative voltage drop $V^{y}_{zz}(17)$ becomes zero at time 31.3 μsec and then turns to be positive. Defining this time as an *inversion time*, we can trace its reciprocal as a function of the current in Fig.10.

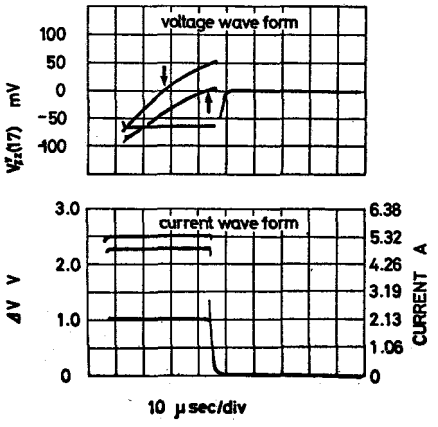

Fig.9 Pulse wave form at 77K under H= 12.5 KG; $V^{y}_{zz}(17)$ for #2 is the voltage drop at angle θ=-59°.

4. Discussion

4.1 Application of Yoshida's model

Yoshida proposed a geometrical transport model such that the inhomogenious current in the *infinite medium* caused by an external electric field E_z and magnetic field H_θ, induces an equipotential line to yield the anomalous field in the x-z plane in the *finite specimen*. Although there remain some suspicious questions as the boundary conditions, the self-consistency of the current density and the electric field, and so on, we carry out making a straightforward application to our present experimental results to see how is the model congruous with the cases in n-InSb. Since the model is based on the compensated metal, it should be used only in n-InSb at room temperature if it is really applicable.

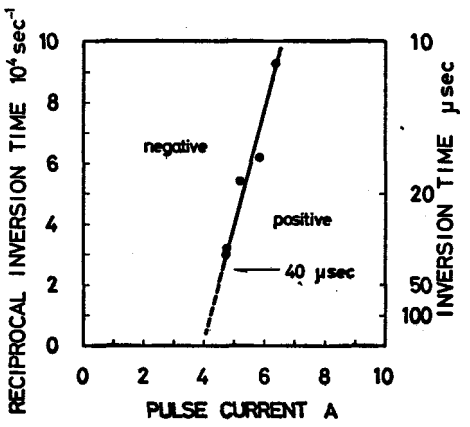

Fig.10 Current dependence of the inversion time, when the negative potential difference turns out positive, for $V^y_{zz}(17)$ of the specimen #2 at an angle θ=-59° and H=12.5 KG at 77K.

One of the purely geometrical problems is concerned with the calculation of θ_d and θ_h. The predictions and the experimental results of Figs 1-8 are compared in Table II, and in Table III from Fig.11, being in considerable agreement with each

Table II. Obseved and calculated values of dip angle θ_d and hump θ_h (degree). The observed values have been taken from Figs.1-8.

specimen	θ_{d+}		θ_{h+}		θ_{d-}		θ_{h-}		
	cal.	obs.	cal.	obs.	cal.	obs.	cal.	obs.	
#2	22	27	41	48 *					Fig.1
	22	24 25	41	47 55					Fig.2
	22	 28	41	 55					Fig.3
#4	17	13	26	30	16	13	25	28	Fig.4
#5					24	(15)	35	53	Fig.7
#6			32	55					Fig.8

* The upper values and the lower values are at 77K and 273K repectively only for #2, and other observed values are at 273K.

Table III. Observed and Calculated values of dip angle θ_d and θ_h (degree). The observed values have been taken from Fig.11, curved from data for #2 measured at 273K.

$V_{zz}^{y}(i,i+1)$	θ_{d+}		θ_{h+}		θ_{d-}		θ_{h-}	
	cal.	obs.	cal.	obs.	cal.	obs.	cal.	obs.
i=1	22	31	41	58	6	-	7	-
2	15	16	22	31	7	-	8	-
3	11	13	15	27	8	-	10	-
4	9	(10)	11	(21)	10	-	14	6
5	7	-	9	(13)	14	-	21	16
6	6	-	7	(8)	21	-	39	31

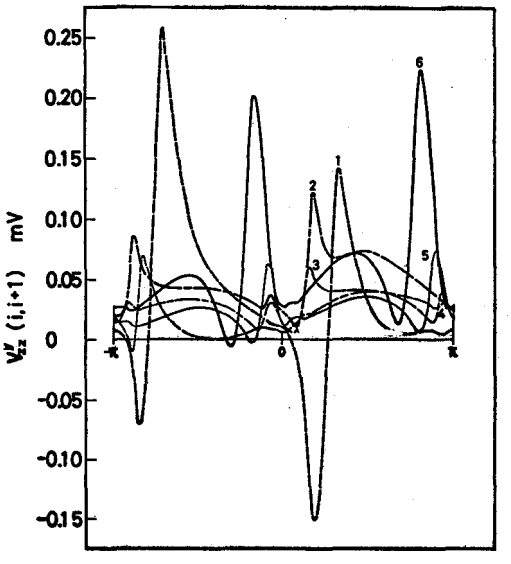

Fig.11 Angular dependence diagram of $V_{zz}^{y}(i,i+1)$ for the terminals i=1-6 for the specimen #2 at 273K under I=1 mA and H=12.5 KG.

other.

Another result from geometrical consideration is a symmetrical relation between the potential differences, $V^{y}_{zz}[\ell^{+},\Delta\ell]_{\theta}=V^{y}_{zz}[\ell^{-},\Delta\ell]_{-\theta}$ where $\ell^{+}=\ell^{-}$. The symmetric fashion of a couple of patterns with respect to $\theta=0^{\circ}$ can be seen in Figs.4 and 11.

Although some of the remarkable trends in the experimental results seem to be self-consistent with Yoshida's geometrical model, further detailed discussion need be cross-examined in n-InSb. It should be marked that the agreements in Table II are fairly well even at 77K.

4.2 On inversion process

One of the most queer phenomena would be the inversion process mentioned in sec. 3.3: Morimoto observed an electromagnetic radiation at this critical point, where the experiments were made via a constant current method at 77K.[5)]

Let us try a speculation to relate this process with the surface recombination. As a matter of fact, lots of unstable problems have been studied extensively so far in these high field region; the pinch effect can be enumerated as one of the verified instabilities in InSb-plasmas, but it may not take place since an external magnetic field is quite strong enough to break the pinching phenomena. It might be also judged from Fig.9 that the acoustic amplification does not progress. Define S as the recombination velocity and $\langle V_y \rangle = (n_i e^2/m_i)\langle\omega_{ci}{}^2\tau_i{}^3/1+\omega_{ci}{}^2\tau_i{}^2\rangle E_z \sin\theta\cos\theta \sim (n_i e^2\tau_i/m_i)E_z\sin\theta\cos\theta$ as the mean velocity of electrons or holes in the y-direction. If $\langle V_y \rangle < S$ is assumed, then the stationary current would be expected in the y-direction in the internal bulk, but the current on the boundary in that direction is of course zero since $I_i - n_i eS=0$ at the surface. Accordingly in this case, the negative field will possibly appear. On the contrary if $\langle V_y \rangle > S$, an accumulation of the relevant charge will cause the electric field in the y-direction to obstruct the further current flow. Assume that the inversion would be due to this accumulation process, and then the reciprocal of an inversion time may be proportional to $\langle V_y \rangle$ since the relaxation time would be dependent on the balance of current flow and diffusion process. But at present stage a clear-cut answer is not known.

Acknowledgement

One of the authors (T.I) wishes to thank Professor Hashimoto for support and encouragement in the course of this study. He is grateful also to Professor Morimoto of Kyoto University for his kind discussion and encouragement, and to H.Maeda for decision of the crystallographic directions of n-InSb wafer by X-ray technique.

References

1) T.Morimoto and K.Yoshida: Proc. 12th LT Conference, Kyoto (1970) 557.
2) T.Morimoto and K.Yoshida: Proc. 13th LT Conference, Boulder (1974) 379.
3) K.Yoshida: J. Phys. Soc. Japan 39 (1975) 1473.
4) T.Morimoto, M.Yamamoto and J.Kawamoto: Phys. Letters 49A (1974) 261.
5) T.Morimoto: Phys. Letters 50A (1974) 183.
6) K.Yoshida: J. Phys. Soc. Japan 40 (1976) 1027.
7) T.Morimoto: private communication, Bull.Inst. Atomic Energy, Kyoto Univ. 44 (1973) 1.